Construction of an In-achromatic Superconducting Wiggler

The Taiwan Light Source was designed to generate photons mainly in VUV and soft X-ray range. However, the need for hard X-rays is growing due to the demand of the users. Superconducting wigglers with high magnetic field can be utilized to extend the photon energy into the hard X-ray range of 10 - 20 keV and to increase the flux by a factor of ten. At TLS, all long straight sections have been already occupied. Hence, an investigation was initiated to study the possibility of installing compact superconducting insertion devices into achromatic sections of the TLS ring to increase the number of hard X-ray sources.

Currently, a 5 T superconducting wavelength shifter is in operation between the two kicker magnets in the injection section and a 3.2 T superconducting wiggler is at downstream of the superconducting RF cavities.

We plan to install a new superconducting wiggler will be installed in the achromatic section of the 6th straight section in 2006. Since the space between the bending magnets is small, an in-achro-matic superconducting wiggler (IASW) with an allowable length of 0.96 m was designed, as shown in Fig. 1. In-achromatic wigglers are not serving as main elements responsible for the electrons circulation in a storage ring. The challenge is not to reduce the reliability of the machine during the wiggler's power-off. Table 1 presents the main parameters of the IASW wiggler.

Magnetic Design

The superconducting wiggler is designed to create the maximum magnetic field strength of 3.1 T with a periodic length of 6.1 cm and a magnet gap of 19 mm. Figure 2 displays the 16-pole magnetic framework of the IASW wiggler.

Table 1: *Main parameters of the IASW wiggler magnet*

Magnetic period	61 mm
Pole gap	19 mm
Vertical beam aperture	11 mm
Horizontal beam aperture	98 mm
Total number of poles	16
Total length of wiggler	960 mm
Peak field	3.1 T
Beam chamber temperature	90 K
LHe boiling off	2 l/h

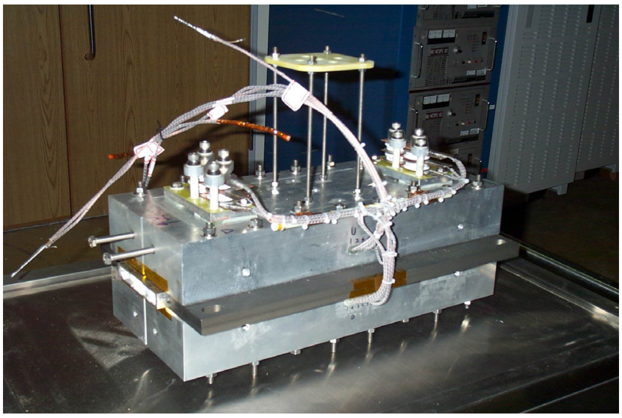

Fig. 2: *The 16-pole framework with protection diode of the IASW magnet.*

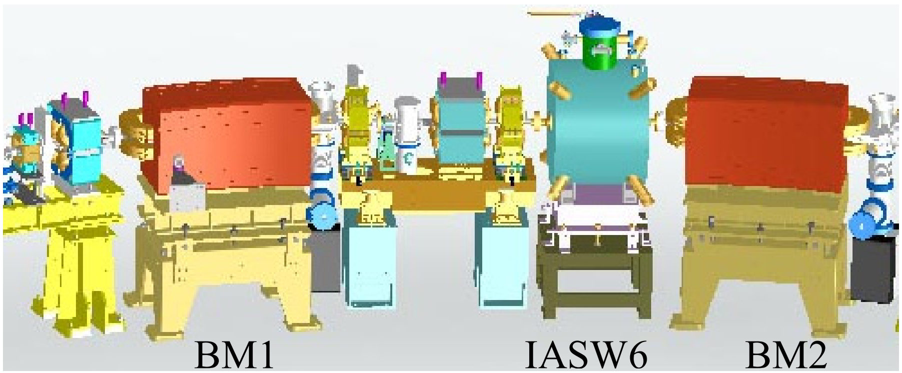

Fig. 1: *Schematic diagram of the IASW wiggler to be installed near the second bending magnet in the triple-bend achromatic section of the storage ring.*

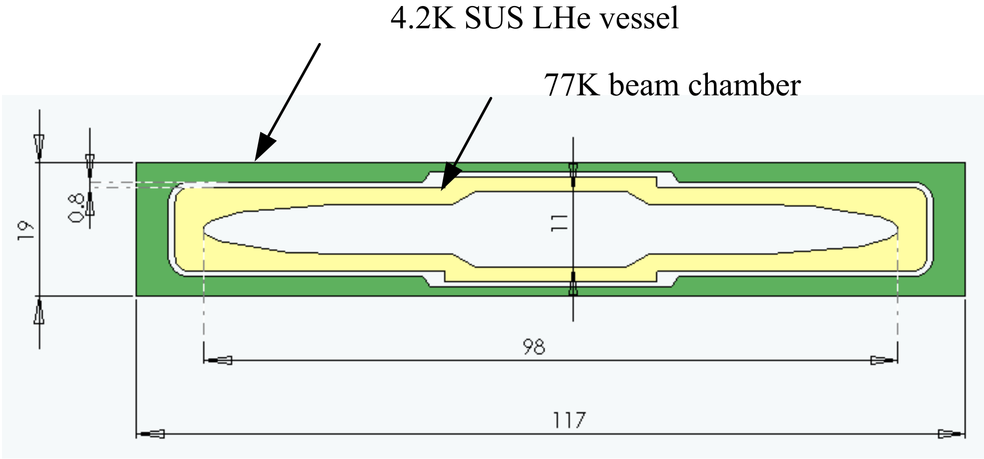

Fig. 3: Schematic cross-section view of the 77 K beam vacuum chamber and the 4.2 K liquid helium vessel (unit: mm).

The superconducting racetrack coil comprises 473 winding turns of 0.64 mm diameter NbTi super-conducting wire. At the maximum field strength of 3.1 T, the soft iron of the pole plates and the yoke near the superconducting coil are fully saturated. The vertical height of the yoke is not sufficient to be saturated at its outside boundaries. The magnetic field strength on the superconducting wire drops significantly when the wire is away from the round curves of the iron pole. Therefore, a clearance of 1.1 mm is left between the pole and the coil with plastic material to reduce the maximum field on the coil, which will increase the tolerance margin space for the magnet design and construction.

The 0.96-meter long wiggler assembly is held in a liquid helium vessel. The wiggler is 500 mm long, 214 mm wide, and 167 mm high with a vertical gap of 19 mm. The vertical gap accommodates a vacuum chamber with horizontal and vertical apertures of 98 mm and 11 mm, respectively. Irradiation from the IASW and the bending magnet hits the vacuum chamber downstream implying that the vacuum chamber of the wiggler needs an inside width of at least 98 mm. A 2mm-thick aluminum vacuum chamber was intercepted with liquid nitrogen to lower the temperature to 90 K. A critical clearance of 0.8 mm is left between the 4.2 K vessel and the 77 K beam duct for thermal shielding.

Prototype Construction and Testing

The IASW wiggler is designed and constructed and the 3-D structure is shown in Fig. 4. A prototype of a five-pole wiggler was manufactured to investigate the mechanical and magnetic field performances. A higher field can be generated by using a holmium pole instead of a low carbon 1006 iron pole. A five-pole prototype magnet was tested and measured using a Hall probe to verify its magnetic field performance in the vertical test dewar. Figure 5 reveals the measured magnetic field strength as a function of the excitation current. The figure reveals

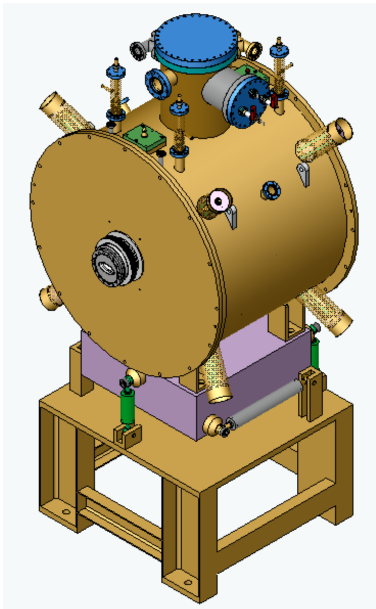

Fig. 4: The 3-D schematic structure layout of IASW wiggler magnet.

that the field strength of the Ho pole is 0.3 T higher than that of the 1006 iron pole. Figure 6 plots the vertical field strength in longitudinal direction. The magnetic structural design and field performance of the proposed wiggler were verified by the designed five-pole prototype.

A winding coil was designed to produce continuous serial 16-pole coils in order to reduce the number of superconducting winding joints. After winding, the coils were assembled with the iron return yoke in an aluminum mold. The superconducting coils were impregnated with epoxy to glue the coil and cured at high temperature of 50^{o} C in the aluminum molds. The compress force clamps from the aluminum mold constrain the coil motion in the beam direction after the magnet cools down. The restraining forces will prevent any significant coil motion, thereby avoiding that the coil quenches.

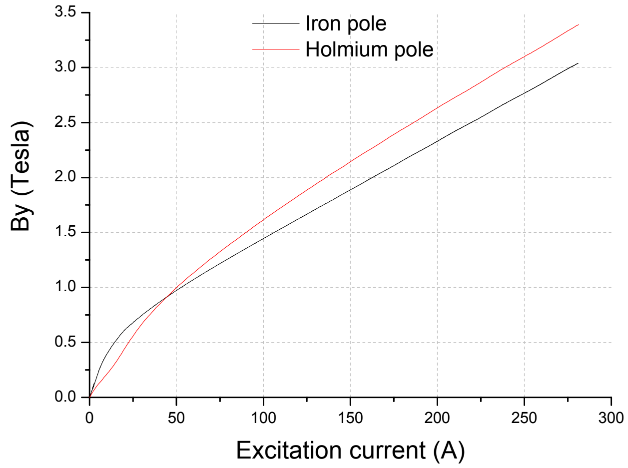

Fig. 5: Measured magnetic field strength as a function of the excitation current.

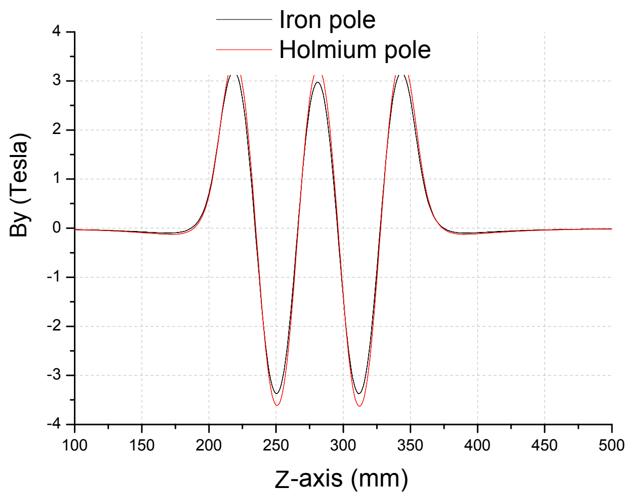

Fig. 6: The measured on-axis vertical field strength along the longitudinal axis of the five-pole prototype IASW. The excitation current is 267 A.

Three pairs of R620 cold diodes were linked across the 16 coils to perform the quench protection. After training the coils repetitively, the magnetic field strengths were evaluated to attain the maximum field of 3.2 T at an excitation current of 270 A. However, the magnet was charged up to 285 A with 3.35 T on the central pole. Figure 7 plots the on-axis vertical field strength in the longitudinal direction. The magnetic structural design and field performance is further evaluated by building a 16-pole prototype with a complete cryostat during the mid-August 2005.

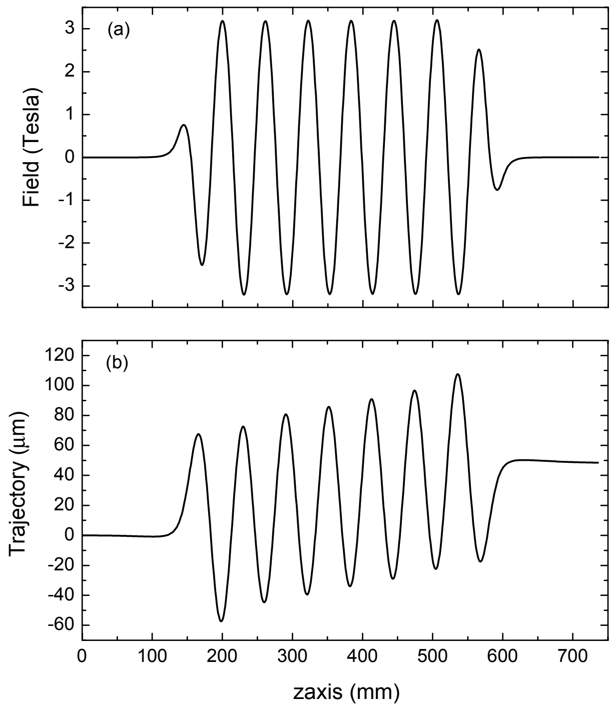

*Fig. 7: **(a)** The measured magnetic field distribution, **(b)** the simulated electron trajectory depending on the measured field, along the longitudinal direction.*

Authors
C. H. Chang, C. S. Hwang, H. H. Chen, F. Y. Lin, M. H. Huang, T. C. Fan, H. C. Liu, and J. C. Jan, National Synchrotron Radiation Research Center, Hsinchu, Taiwan

Contact e-mail
chang@nsrrc.org.tw